

Supplemental Information

Inventory of Supplemental Information

Figure S1. Related to Figure 1, to show 3-D images of nerve/vessel patterning.

Figure S2. Related to Figure 3, to validate Npn-1 signaling is not involved in Sema3E/Plexin-D1 signaling.

Figure S3. Related to Figure 5, to validate the sensitivity of AP-ligand binding assay.

Figure S4. Related to Figure 6, to show detail quantitative analysis of nerve and vessel ring distance from center of each whisker follicles

Figure S5. Related to Figure 7, to show potential attractive cues to establish double ring structure.

Figure S6. Related to Figure 7, to show *in vivo* evidence of nerve ring formation by NGF

Movie S1. Related to Figures 1 and S1, to show 3-D images of nerve/vessel patterning at E12.5

Movie S2. Related to Figures 1 and S1, to show 3-D images of nerve/vessel patterning at E14.5

Movie S3. Related to Figures 1 and S1, to show 3-D images of nerve/vessel patterning at E16.5

Supplemental Figures

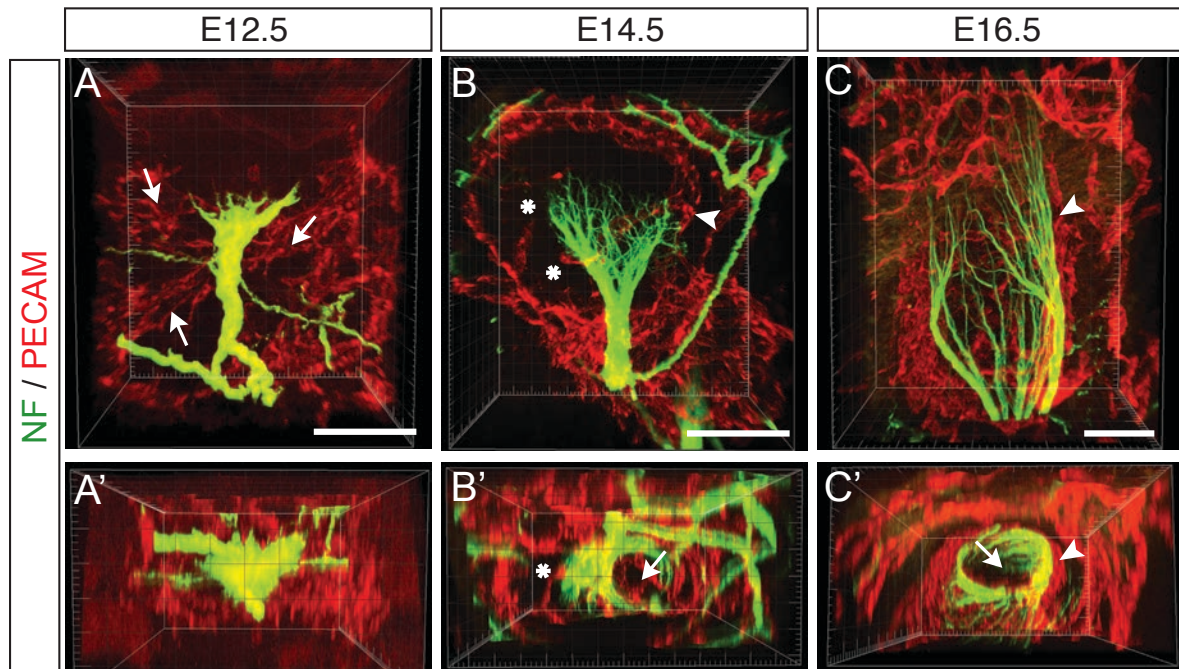


Figure S1. Three-dimensional imaging analysis of nerve/vessel ring organization during development. Vessel and nerve were visualized by PECAM and NF immunostaining with thick sections taken from whisker follicles during “double ring” organization (A-C, lateral view; A'-C', top view). (A-A') At E12.5, blood vessels appear to be randomly positioned surrounding the TG nerve shaft (arrows in A). (B-B') Around E14.5, vessels begin to remodel to organize the “double ring” structure. While the TG nerve forms a clear ring structure (arrow in B'), some blood vessels are apart from the nerve shaft (asterisks in B) and others are still located closely to TG nerves (arrowhead in B). (C-C') At E16.5, blood vessels are aligned with the nerve ring (arrow in C') to establish an outer blood vessel ring (arrowhead in C and C'). Scale bar: 40 μm (A-C)

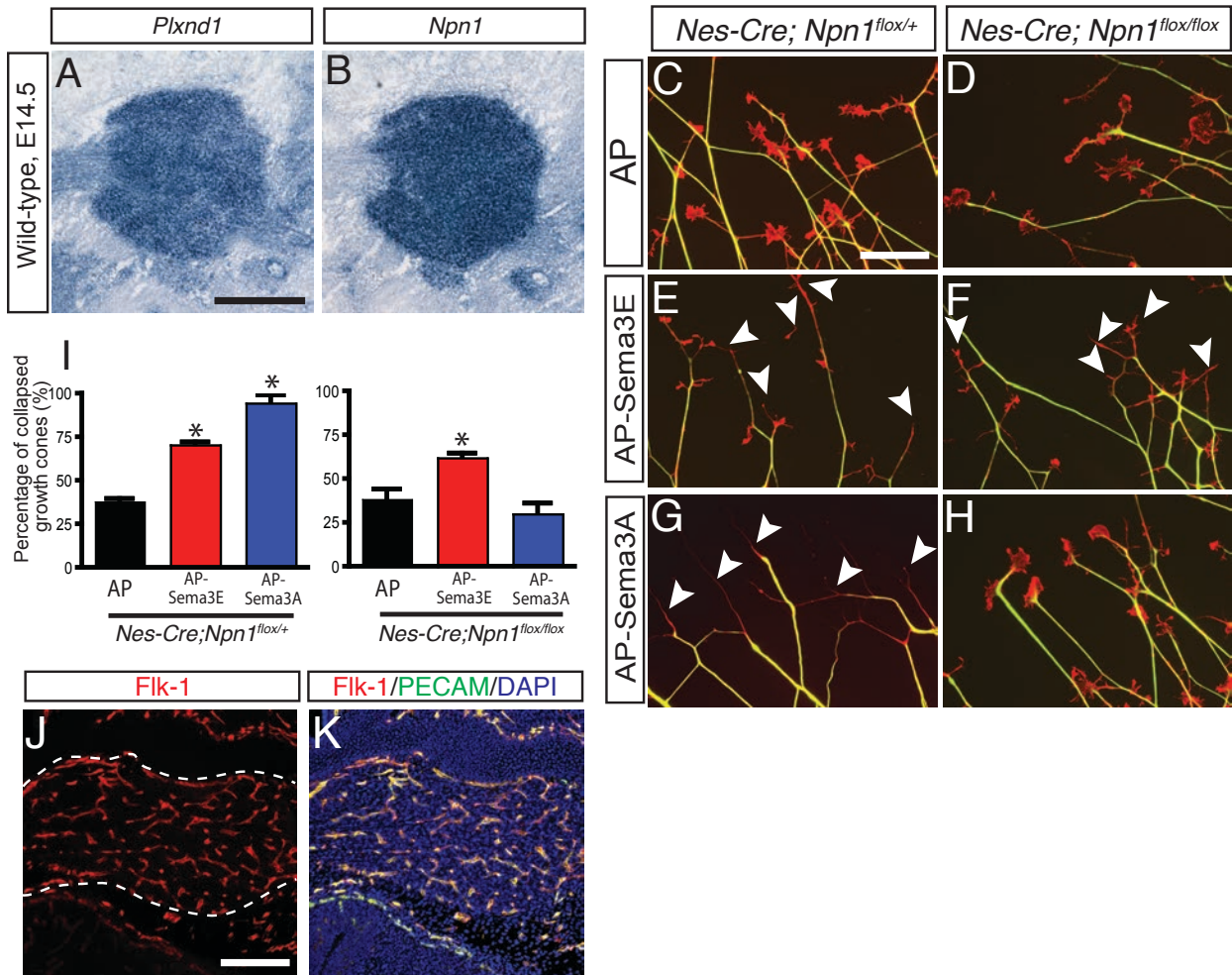


Figure S2. Neuropilin-1 is not required for Sema3E-Plexin-D1 signaling-mediated trigeminal growth cone collapse. (A-B) *Npn1* and *Plxnd1* ISH on adjacent sections of wild-type embryos at E14.5 shows that *Npn1* mRNA is also significantly expressed in the TG at E14.5. (C-H) Sema3E induces TG growth cone collapse in the absence of Npn-1. The TG growth cone collapse assay was performed as described in Fig 2J-Q, using TG isolated from *Nestin-cre; Npn1^{fllox/fllox}* (D, F, H) mutant mice that lack Npn-1 in trigeminal neurons, or from littermate control mice *Nestin-Cre; Npn1^{fllox/+}* (C, E, G). Sema3A treatment (2 nM of AP-Sema3A) induces TG growth cone collapse in the control (arrowheads in G), but Npn-1 mutant growth cones are resistant to collapse (H).

However, Sema3E treatment (2 nM of AP-Sema3E) leads to a similar level of growth cone collapse in the control and Npn-1 mutant mice (arrowheads in E and F). **(I)** Quantification of the growth collapse. Experiments were performed in triplicate and values shown are mean \pm SD. For statistical analysis, one way ANOVA, Newman-Keuls multiple comparison test was performed and values that have a $P < 0.001$ are marked with an asterisk. **(J-K)** Flk-1 and PECAM double immunostaining at E14.5 shows that Flk-1 protein is only detected in blood vessels located in the TG (dotted area), not in the TG neurons. Scale bar: 500 μ m in A applies to B, 50 μ m in C applies to H, and 200 μ m in J to K.

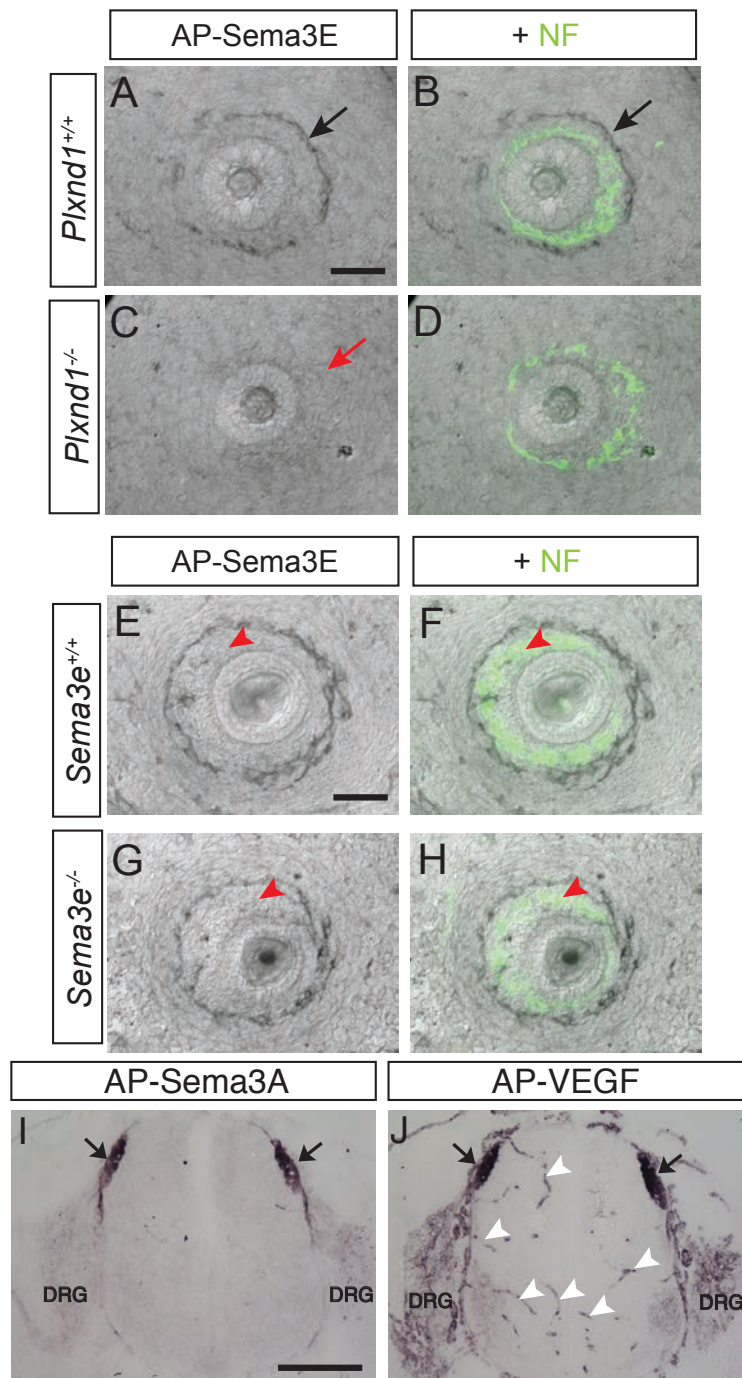


Figure S3. AP-Sema3E specifically binds to Plexin-D1 and endogenous Sema3E does not interfere AP-Sema3E binding to trigeminal nerves. (A-D) AP-Sema3E binds to the blood vessel ring in E14.5 wild-type whisker follicles (black arrow in A and B). In the *Plxnd1* null embryo, AP-Sema3E does not recognize Plexin-D1 even in the blood vessel (red arrow in C). **(E-H)** AP-Sema3E binding on the nerve ring is not

enhanced in the Sema3E null whisker follicle. AP-Sema3E does not detect Plexin-D1 in the nerve ring from E16.5 wild-type embryos (red arrowhead in E and F). Likewise, ablation of endogenous Sema3E does not help to increase AP-Sema3E sensitivity detecting Plexin-D1 (red arrowhead in G and H). **(I-J)** AP-Sema3A and AP-VEGF ligands (2nM) were applied to transverse sections of spinal cord in E11.5 embryos. Whereas AP-Sema3A only recognizes nerves in dorsal root entry zone (black arrows in A), not blood vessels in spinal cord, AP-VEGF detects both nerves and blood vessels (black arrows and white arrowheads in B). Scale bar: 50 μm (A-H), 200 μm (I-J).

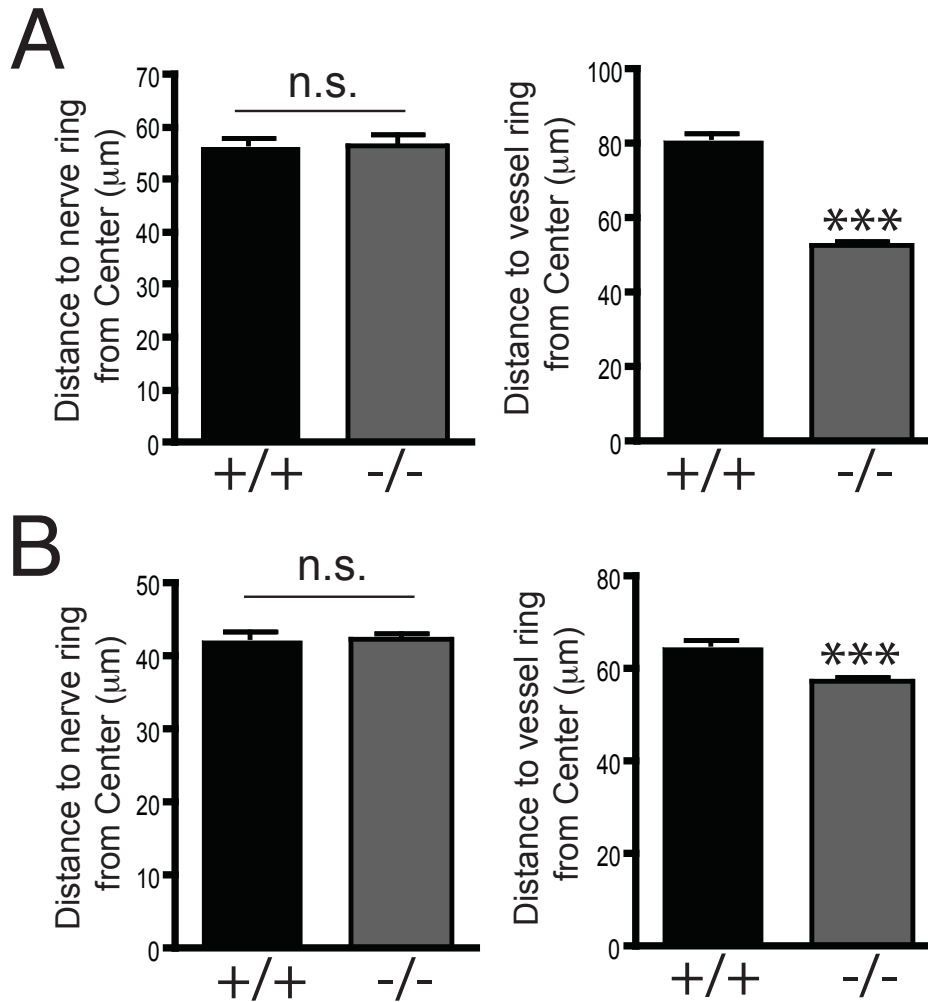


Figure S4. Quantitative analysis of nerve and vessel ring distance from whisker center. (A) Nerve ring and vessel ring distance from center was measured in individual paired follicles from Plexin-D1 mutants and littermate controls. While nerve ring distance from each pairs shows no difference (left graph), vessel ring distance in the mutant is dramatically decreased (right graph) compared to control. Quantification is shown as mean \pm SEM (n=12 paired follicles from three different litters). (B) Sema3E null mice also show the similar nerve/vessel ring distance patterns. Quantification is shown as mean \pm SEM (n=9 paired follicles from three different litters). Paired student *t*-test; ***, $P < 0.001$; n.s, not significant.

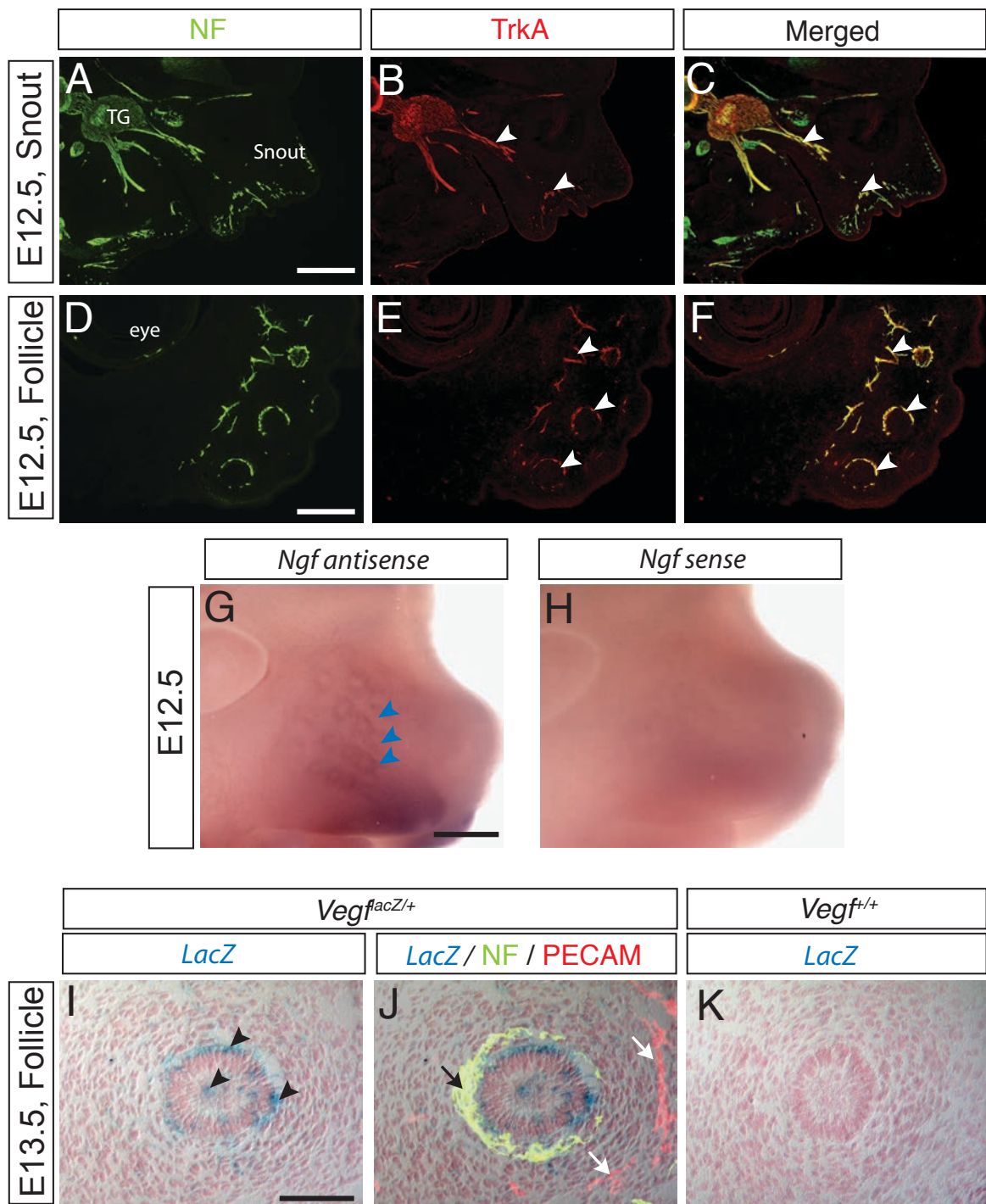


Figure S5. NGF and VEGF are expressed in the whisker follicle when the TG nerves and neighboring blood vessels begin to form ring-like structure. (A-F) The NGF receptor, TrkA is expressed in the innervating trigeminal axons. NF (A and D) and TrkA (B and E) immunostaining is performed at E12.5 and TrkA is highly expressed in the

trigeminal axons projecting to the snout (arrowheads in B and C) as well as axon terminals surrounding whisker follicle (arrowheads in E and F). **(G-H)** NGF is expressed at the whisker follicle. Whole-mount ISH of *Ngf* at E12.5 shows that *Ngf* mRNA is specifically detected around the whisker follicle (blue arrowheads in G) compared to control ISH with sense riboprobe (H). **(I-K)** VEGF is expressed in the whisker follicle areas. VEGF expression is visualized by LacZ staining using heterozygous *Vegf^{lacZ}* reporter mice in which β -galactosidase with a nuclear localization signal is expressed under the control of the VEGF promoter. The majority of LacZ-positive cells are localized in the central area of whisker follicle and some sparse labeling is seen in surrounding tissues (black arrowheads in I) at E13.5. To see the relative location of nerves and vessels, NF (black arrow) and PECAM (white arrow) immunostaining was performed on an adjacent section and overlaid (J). No LacZ-positive cells were detected in the wild-type embryos (K). Scale bar: 500 μm (A-C and G-H), 200 μm (D-F), and 50 μm (I-K).

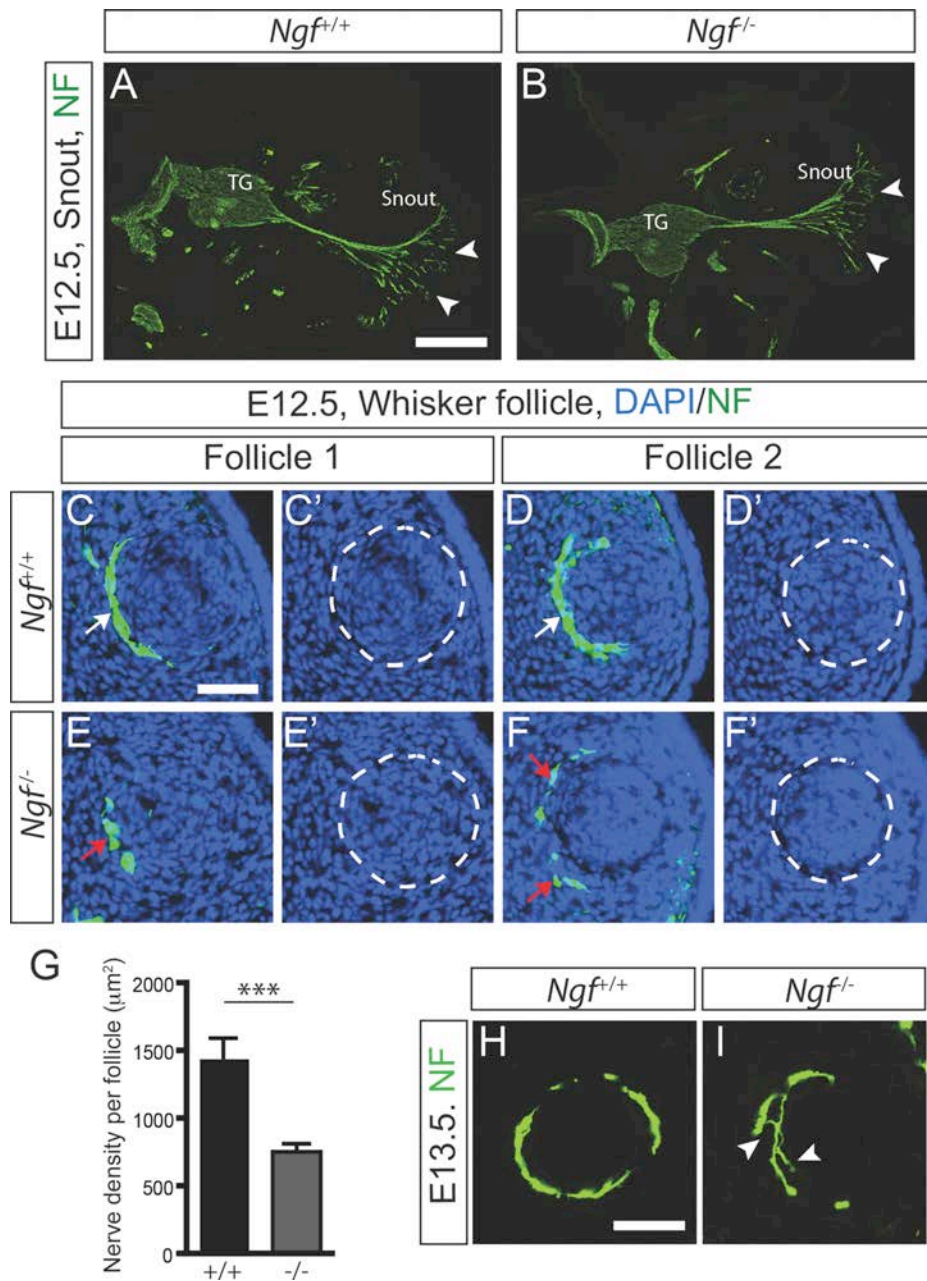


Figure S6. NGF is required for initial whisker nerve ring formation *in vivo*.

(A-B) Normal peripheral projections of trigeminal nerves to the snout area in *Ngf* knockout mice (arrowheads in B) and their littermate controls (arrowheads in A). **(C-G)**

Initial nerve ring formation at the whisker primordium is aberrant in E12.5 embryos lacking NGF. Two representative follicles of *Ngf* knockouts (E and F) and littermate controls (C and D), respectively. In the wild-type embryos, nerves are tightly fasciculated and begin to form ring shape (white arrows in C and D). However, *Ngf* knockout embryos fail to form clear ring shapes surrounding whisker primordium and have fewer fasciculated nerve bundles (red arrows in E and F). (G) Quantification of nerve ring density in the each whisker primordium (mean \pm SEM, n=11). Mann-Whitney test; ***, $P < 0.001$. (H-I) Defects of nerve ring formation are maintained at E13.5 (arrowheads in I). Scale bar: 500 μm (A-B), 50 μm (C-F and H-I).

Supplemental Experimental Procedures

Wholemout immunostaining and 3-D analysis

For wholemount whisker follicle staining, embryos were fixed in 4% PFA in 0.1M phosphate buffer (pH7.5) for 6 hrs and equilibrated in 30% sucrose at 4°C overnight. Embryo snout areas were sectioned in a direction parallel to the whisker follicle at 200-300 μ m using a cryostat (Leica) and washed in 1X PBS containing 0.3% Triton X-100 (PBST) for 1 hr. Sections were then blocked in 1X PBST containing 10% dimethylsulfoxide and 5% normal goat serum for 3 hrs and incubated with primary antibodies in blocking buffer at room temperature for 2 days. The antibodies used were: α -neurofilament (1:50; 2H3) and PECAM (1:500). After washing in 1X PBST for 1 hr five times, sections were incubated in AlexaFluor conjugated secondary antibodies (1:500, Invitrogen) diluted in blocking buffer for 1 day, then washed several times and dehydrated with 100% methanol. Before mounting, sections were cleared with benzyl alcohol and benzyl benzoate mixture. Sections were analyzed by confocal laser-scanning microscopy using a Zeiss LSM 510 META and 3-D images were constructed and analyzed using Imaris X64 software (version 6.4.2.).

Immunohistochemistry

For Flk-1 (VEGFR2) immunohistochemistry, embryos were fixed in 4% PFA in 1 X PBS (pH 7.5) for 2 hr and equilibrated in 30% sucrose at 4°C overnight. The antibodies used are: α -VEGFR2 (1:2000; AF644, R&D Systems) and α -PECAM (1:500; 553370, BD Pharmingen™). All staining procedures were performed as described in “Experimental

Procedures". After final washes, sections were mounted with Prolong Gold antifade reagent with DAPI (Molecular Probes).

Whole mount *in situ* hybridization

Whole mount *in situ* hybridization was performed on E12.5 day old embryos. Embryos were fixed in 1XPBS/0.1% Tween20 (PBST) containing 4% PFA overnight at 4°C. Then samples were serially dehydrated in methanol, rehydrated in PBST, bleached in 4:1 PBST/30% hydrogen peroxide for 1 hr, incubated in 10 µg /ml proteinase K in PBST for 20 min, and fixed again in 0.2% glutaraldehyde/4% PFA in PBS. After several washes in PBST, embryos were pre-hybridized in hybridization buffer (50% formamide, 5X sodium citrate solution (SSC), pH 5.0, 50 µg/ml yeast total RNA, 1% SDS, 50 µg/ml heparin) at 65°C and hybridized in antisense or sense riboprobes of *Ngf* (ENSMUST00000035952, nt 170-890) overnight. After several serial washes in these washing buffers (solution 1: 50% formamide, 5X SSC pH 5.0, 1%SDS; solution 2: 0.5 M NaCl, 10 mM Tris-HCl pH 7.5, 0.1% Tween 20; and solution 3: 50% formamide, 2X SSC pH 5.0), samples were incubated to anti-DIG antibody binding in Tris-buffered saline containing 0.1% tween 20 (TBST) overnight at 4°C. After incubation, samples were washed several times for 1 hr each in TBST and then twice for 30 min each in alkaline phosphatase buffer containing 2 mM levamisole. To visualize positive signals, samples were incubated with BM Purple (Roche) precipitating substrate.

LacZ staining

Staining for β-galactosidase (lacZ) was performed according to standard method with

minor modifications (Nagy et al., 2003). Briefly, fresh frozen sections were fixed in 0.4% paraformaldehyde (PFA), 100 mM PIPES (pH 6.8), 2 mM MgCl₂, 5 mM EGTA for 10 minutes. They were rinsed in 1X PBS (pH 7.3), 2 mM MgCl₂, 0.01% sodium deoxycholate, 0.02% Igepal and stained in 1X PBS containing 2 mM MgCl₂, 0.01% sodium deoxycholate, 0.02% Igepal, 5 mM potassium ferricyanide, 5 mM potassium ferrocyanide, and 1 mg/ml X-gal at 37 °C until a clear blue precipitate was visualized. After staining, embryos were washed in PBS, post-fixed in 4% PFA/PBS for 5 min at room temperature, and counterstained with nuclear fast red before mounting. Adjacent sections were processed according to standard immunostaining with anti-NF and PECAM antibodies described in “Experimental Procedures”. To visualize the nerve/vessel ring, immunostaining images were overlaid on LacZ staining images using Photoshop.

Supplemental References

Nagy, A., Gertsenstein, M., Vintersten K., and Behringer R. (2003). *Manipulating the Mouse Embryo* (New York: Cold Spring Harbor Laboratory Press)